2019-07-01

Bottom-Up Controls (Micronutrients and N and P Species) Better Predict Cyanobacterial Abundances in Harmful Algal Blooms Than Top-Down Controls (Grazers)

Scott Andrew Collins

Bottom-Up Controls (Micronutrients and N and P Species) Better

Predict Cyanobacterial Abundances in Harmful Algal Blooms

than Top-Down Controls (Grazers)

Scott Andrew Collins

A thesis submitted to the faculty of
Brigham Young University
in partial fulfillment of the requirements for the degree of

Master of Science

Zachary T. Aanderud, Chair
Benjamin W. Abbot
Michelle Baker
Greg Carling
Neil Hansen

Department of Plant and Wildlife Sciences

Brigham Young University

ABSTRACT

Bottom-Up Controls (Micronutrients and N and P Species) Better
Predict Cyanobacterial Abundances in Harmful Algal Blooms
than Top-Down Controls (Grazers)

Scott Andrew Collins
Department of Plant and Wildlife Sciences, BYU
Master of Science

The initiation, bloom, and bust of harmful Cyanobacteria and algae blooms (HAB) in lakes are controlled by top-down and bottom-up ecological controls. Excess phosphorous and nitrogen inputs from anthropogenic sources are primary to blame, but eukaryotic grazers may also promote or curb Cyanobacteria dominance. We tracked shifts in bacterial composition, lake chemistry, and eukaryotic grazing community weekly or bi-weekly through spring and summer and modeled the causes of specific Cyanobacterial species blooms and busts across three lakes in Utah, USA, with differing lake trophic states. Regardless of trophic status, all three lakes experienced blooms of varying composition and duration. *Aphanizomenon* strain MDT14a was the most dominant species in every bloom on Utah Lake, comprising up to 44.16% of the bacterial community. Utah Lake experienced a total of 18 blooms across all sites ranging in duration from one to six weeks. *Phormidiaceae sp.* (8.5 ± 6.1%) and *Microcystis sp.* (9.7 ± 4.7%) were the most abundant species in the Deer Creek bloom. Deer Creek experienced one bloom at the beginning of fall. *Nodularia sp.* (9.7 ± 2.1) dominated Great Salt Lake bloom. The Great Salt Lake experienced four separate blooms during the summer months that lasted one to three weeks. Phosphorous concentrations on Utah Lake varied across site and season. Nitrate concentrations on Deer Creek increased over season with a ten-fold increase in concentration. We characterized Cyanobacteria blooms as either bloom communities (growing populations of Cyanobacteria) or as bust communities (declining populations of Cyanobacteria). Using these designations, we modeled the growth and decline of the Cyanobacteria populations across season with top-down and bottom up-controls. Based on generalized least-squared modeling, eukaryotic grazing does not affect relative Cyanobacteria abundances as much as nutrient limitations. *Aphanizomenom* strain MDT14a was positively correlated with temperature ($P < 0.028$) and the concentration of K ($P = 0.007$) and negatively correlated with increases in conductivity ($P = 0.0088$). *Microcystis* was positively correlated with increasing levels of SRP ($P < 0.001$) and negatively correlated with higher Ca concentrations ($P = 0.008$) and PP ($P = 0.008$). Busts of *Microcystis* were related to decreases in nitrate ($P = 0.06$) and lower total lake depths ($P = 0.03$). *Phormidiaceae sp.* relative abundance was negatively correlated with higher levels of TDN ($P = 0.01$-0.001) and Mg ($P = 0.01$) and positively correlated with higher S concentrations ($P = 0.007$). Our findings suggest that micronutrients and more bioavailable forms of P may potentially allow Cyanobacteria to break dormancy and proliferate HAB communities.

Keywords: cyanobacteria, Utah Lake, generalized least squared models, bacterial and eukaryotic rDNA communities, top-down bottom-up controls

TABLE OF CONTENTS

LIST OF FIGURES

LIST OF TABLES

INTRODUCTION

The initiation, bloom, and bust of harmful cyanobacteria and algae blooms (HABs) potentially occurs due to shifts in multiple lake physiochemical conditions (Paerl and Otten, 2013), meteorological background (Zhang et al., 2016), and trophic interactions (Ger et al., 2014; Haney, 1987). HABs are an ecological phenomenon controlled by both bottom-up nutrient concentrations especially phosphorus (P) as well as top down herbivory controls. Excess nutrients from human activity trigger cyanobacterial blooms, which may create expansive hypoxic dead zones in lakes that damage ecosystems, hurt local economies, undermine food and water security, and directly harm human health (Brooks et al., 2016). HABs worldwide are becoming more prolific correlating with the 500% increase in global fertilizer use over the last 50 years while land use change is resulting in contamination of surface waters through non-point sources (Abbott et al., 2018; Foley et al., 2011; Pinay et al., 2015; Seitzinger et al., 2010). As with the intensification of bottom-up controls, common eukaryotic grazing organisms such as copepods, calanoids, rotifers, ciliates, and cladocerans influence HAB intensities. Zooplankton grazing predominantly curbs HABs by either selectively feeding on individual species of cyanobacteria or by indiscriminately feeding on the total cyanobacteria populations regardless of species... Encapsulated within all HABs and top-down and bottom-up controls are a potential myriad of cyanobacterial species that may individually bloom and become dominant or bust and return to being rare or enter a state of dormancy. Ultimately, HABs are inherently complicated being dominated by a single species or a cohort of species responding to a cadre of environmental factors and acting as the primary producers of lake food webs (Randall et al., 2019; Wood et al., 2017).

The importance of nutrients in regulating HABs is significant, however, nutrients resources are often coarsely measured and Cyanobacterial species are haphazardly lumped together. Total Cyanobacteria or algal biomass is classically related to the absolute amount of P or N, rendering an inaccurate causal relationship between Cyanobacteria and resource availability in eutrophying systems. Multiple forms of P and N exist in freshwater lakes, each with varying degrees of bioavailability, solubility, and sediment geochemistry potentially influencing HABs in vastly different ways (Descy et al., 2016; Heisler et al., 2008; Song et al., 2017). In conjunction with nutrient bioavailability, species of Cyanobacteria demonstrate preference for different N and P forms. These preferences are dictated by microbial traits and life-history strategies developed over evolutionary time. For example, often dominant contributors to HABs, Aphanizomenom flos-aqaue proliferates in the presence of the highly-available, dissolved inorganic P, whereas, Nodularia spumigena relies extensively on intracellular P storage and remineralization of organic phosphorous (Vahtera et al., 2007). Also, when inorganic N is limiting, N-fixing species with heterocysts, such as Aphanizomenon and Dolichsospermum spp. may proliferate and dominate. Conversely, when inorganic N is not limiting, non-heterocystous cyanobacteria, such as Microsystis and Plankthorix spp. may out compete N-fixing species (Moisander et al., 2003; Paerl and Otten, 2013). Additionally, several trace nutrients such as Fe, Zn, Mn, Co, and Cu are required for cyanobacteria metabolic function and are often overlooked (Bonilla et al., 1990; Downs et al., 2008; Heisler et al., 2008; Paerl and Fulton, 2006). For example, Fe is essential for cyanobacterial growth because it is a required for several processes such as photosynthesis, N assimilation, and N fixation (Paerl and Fulton, 2006). Regardless, nutrients are consistently framed as factors eliciting HABs but rarely causing blooms to decline or bust. The goal to mitigate HABs often rely heavily on nutrient control (Paerl and Otten, 2013), but it's unclear if a

decline in lake nutrient concentrations due to bacterial consumption of resources or a decline in resource inputs cause a decline in certain cyanobacterial species while its blooming. If bottom-up control measurements embrace the importance of nutrient form and micronutrients as well as identify the triggers for bloom growth and decline, a more complete contextual basis for HABs may emerge.

Even with the importance of top-down and bottom-up interactions in structuring HABs, rarely are these two ecological triggers evaluated simultaneously to explain blooms and busts of cyanobacteria. Multiple eukaryotic grazers prey on cyanobacteria (Work, 2003), but multiple other ecological phenomenon may exist in lake food webs that affect cyanobacteria populations. In a mesotrophic lake in Wisconsin USA, Daphnia grazing slowed down or even prevent the growth of inedible filamentous cyanobacteria during the summer months (Kâ et al., 2012; Sarnelle, 1993). Furthermore, zooplankton grazing reduces N-fixation processes of filamentous cyanobacteria by reducing filamentous length, which decreases N-fixation rates by 40%, ultimately controlling the growth of the Cyanobacteria (Chan et al., 2004). In general, cyanobacteria are a poor nutrient source for zooplankton and may either produce toxins or contain intracellular toxins causing zooplankton to selectively graze on algae, but selective grazing may facilitate the bloom of marginalized cyanobacterial species (Work, 2003). This phenomenon is known as the 'predation release' or 'ecological release' hypothesis. The ecological release hypothesis states that when a given species is freed from specific limiting factors such as competition or grazing pressure, the species population may dramatically increase. Additionally, Cyanobacterial growth form may also influence grazing potential. For example, colonial or filamentous growth of certain cyanobacterial species may render the species

inedible by eukaryotic grazers because they become too large to ingest and may even disrupt feeding behavior (Gilbert and Durand, 1990).

To examine the top-down and bottom-up controls on individual cyanobacteria species, we tracked HABs weekly or bi-weekly over the spring and summer across three lakes in Utah, USA, with differing lake trophic states. We evaluated shifts in bacterial HAB communities through 16s rRNA gene target-metagenomics, classified cyanobacterial species blooms and busts based on relative abundance and direct cell counts, and modeled the potential for differing forms of N and P, lake physiochemistry, and eukaryotic grazer community compositions to trigger and sustain cyanobacterial blooms and busts. We selected Utah Lake (eutrophic), Deer Creek Reservoir (mesotrophic), and Great Sale Lake, Farmington Bay (hypereutrophic conditions) during the spring and summer of 2017) to represent three trophic states. We hypothesized that: 1) the availability of bioavailable N (NH_4^+ and NO_3^-) and/or P (SRP) will regulate species-specific Cyanobacterial blooms and busts regardless of lake trophic state; 2) micronutrients involved in Cyanobacterial metabolism and photosynthesis will influence specific cyanobacteria but to a lesser extent than bioavailable forms of N and/or P; and 3) certain species of grazers will predominantly relate to the busts of individual Cyanobacteria species. We excluded algae and diatoms species form our study but acknowledge that they are part of blooms and are sensitive to chemistry. We focused however; on Cyanobacteria since the deleterious effects of harmful algal blooms (HAB) arise from Cyanobacteria breaking dormancy, growing, becoming dominant, and producing cyanotoxins.

MATERIALS AND METHODS

Lakes and Sampling

We sampled waters from three lakes across the Wasatch Front in Utah, USA in the late spring through early fall (5 May–October 10, 2017). We selected the lakes primarily to create a gradient of nutrient availability with Utah Lake(40.2130° N, 111.8025° W) classified as eutrophic, Deer Creek Reservoir (40.4453° N, 111.4962° W) as mesotrophic, and the South Arm of the Great Salt Lake, Farmington Bay(41°02'12.8"N 112°09'12.5"W) as eutrophic/hypereutrophic. We also selected the lakes to form a salinity gradient with salinity, as log practical salinity units, in the lakes over the spring and summer (measured monthly as follows: Utah Lake = 0.56 ± 0.07, Deer Creek Reservoir = -0.43 ± 0.03, and Great Salt Lake = 5.2 ± 0.71. We measured a wide range of environmental conditions concurrently with bacterial sampling to identify which parameters correlated with shifts in cyanobacterial blooms and busts. We measured water temperature, pH, electrical conductivity, barometric pressure, and dissolved oxygen (DO) *in situ* using a multiparameter sensor (YSI EXO) in the top 30 cm of the water column. We measured secchi depth and total depth at each site. For each sample date and location, we collected three composite water samples, consisting of three 1 L subsamples from the surface to a depth of 30 cm. One composite sample was filtered to remove bacterial biomass using 0.2 μm pore size filters (Supor PES membrane, Pall Life Sciences, Port Washington, NY,USA) in Nalgene Filter cups and the filters were placed immediately on dry ice. The second composite sample was filtered through 0.45 μm filters (SuporR PES membrane, Pall Life Sciences, Port Washington, NY,USA) and placed on ice. The third set of composite samples were collected without filtration and were placed on ice. All of the samples were transported

back to the laboratory within hours of sampling and stored at -20∘C for nutrient and DNA

analyses.

Lake Chemistry

We analyzed four forms of P, three forms of N, and nine micronutrients as data to inform our

modelling efforts to predict cyanobacterial blooms and busts. The five forms of P vary in

reactivity and potential bacterial use, with the forms including and total phosphorus (TP), a

conglomerate measurement of P in both organic and inorganic forms; total dissolved P (TDP), a

conglomerate measurement of dissolved organic and inorganic P; particulate phosphorous (PP),

P bound to colloids or assimilated within other organisms and presumed to be relatively

unavailable to cyanobacteria; dissolved organic P (DOP), indicative of recently released material

from plant tissue, manure, and other biological sources of phosphorous; and soluble reactive P

(SRP), an inorganic form of P, mostly orthophosphate, that is the most bioavailable to bacteria.

Briefly, we analyzed: TP concentrations by using a nitric acid microwave assisted digestion

followed by determination with a Thermo Scientific ICP-OES (iCAP 7400, Thermo Electron,

Madison, WI, USA; ref); SRP with the ascorbic acid method (ref); and TDP on a Thermo

Scientific ICP-OES (iCAP 7400, Thermo Electron, Madison, WI, USA; ref). We calculated PP

using the formula TP – TDP and DOP with TDP – SRP. The three forms of N included

ammonium (NH_4^+), nitrate (NO_3^-) and total dissolved N (TDN). We analyzed, Ammonium-N

and Nitrate-N using a flow injection analysis on a rapid flow analyzer (Quick Chem 8500,

Lachat Instruments, Loveland, Colorado, USA). Nitrate-N concentrations were determined using

the cadmium reduction method, and the Ammonium-N concentrations were determined using the

sodium salicylate-sodium nitroprusside method. TDN was analyzed with catalytic thermal

decomposition/chemiluminescence method on a Shimadzu TOC analyzer (TOC/TN-L, Shimadzu Scientific, Kyoto, Kyoto Prefecture, Japan). Major cations (i.e., K, Mg, Mn, S, and Zn) and other trace elements (i.e., B, Ca, Cu, Fe), which potentially shape bacterial community structure (Zeglin, 2015), were measured using an Thermo Scientific ICP-OES (iCAP 7400, Madison, Wi, USA). We also evaluated dissolved organic carbon (DOC) determined by acidification or sparging of inorganic carbon followed by combustion catalytic oxidation and NDIR detection on the Shimadzu TOC analyzer (TOC/TN-L, Shimadzu Scientific, Kyoto, Kyoto Prefecture, Japan). Although DOC is not necessarily a nutrient for cyanobacteria, we used the metric as a surrogate for total bacterial biomass.

Bacterial and Eukaryotic Communities Inferred from rDNA

We characterized lake cyanobacteria from bacterial communities and potential eukaryotic grazer communities using a dual-indexed target metagenomic sequencing approach (Kozich et al., 2013). We extracted lake genomic DNA from the 0.2µm filters using the DNEasy PowerWater Kit (Qiagen, Valencia, CA, USA). For bacterial communities, we PCR-amplified the V4 region of the 16S rRNA gene with primer set 515F and 806R , using thermal cycle conditions of an initial denaturation at 95°C for 5 minutes, followed by 35 cycles of denaturation at 95°C for 20 seconds, annealing at 55°C for 30 seconds, and extension at 72°C for 2 minutes, followed by a final extension of 72°C for 3 minutes. For eukaryotic communities, we PCR-amplified the V9 region of the eukaryotic 18S rRNA gene with primer set 1391f and EukBr , following the same thermal cycle conditions after adjusting the annealing temperature to 55.6°C. The barcoded samples were purified and normalized with a SequalPrep Normalization Plate Kit (Invitrogen, Carlsbad, CA, USA); pooled at approximately equimolar concentrations; further

purified using the DNA Clean & Concentrator-25 kit (Genesee Scientific, San Diego, CA, USA), and quantified with an Agilent 2100 Bioanalyzer (Agilent, Santa Clara, CA, USA). All samples were sequenced at the Brigham Young University DNA Sequencing Center (http://dnasc.byu.edu/) via 2×250bp paired-end sequencing at on an Illumina HiSeq 2500 System. We analyzed all sequences using mothur (v. 1.29.2), an open-source, expandable software pipeline for microbial community analysis(Schloss et al., 2009). After removing barcodes and primers, we screened sequences to parse out short reads, chimeras, and non-bacterial sequences. We eliminated short sequences by removing any sequence < 250 bp in length and any sequence with a homopolymeric runs longer than 8 bp. We denoised the sequences with Amplicon Noise (Quince et al., 2011). We removed chimeras using UCHIME (Edgar et al., 2011) and eliminated chloroplast, mitochondria, archaeal, and eukaryotic 16S rRNA gene sequences based on reference sequences from the Ribosomal Database Project (Cole et al., 2009). We then aligned sequences against the SILVA database (Pruesse et al., 2007) using the SEED aligner and then we created operational taxonomic units (OTUs) based on uncorrected pairwise distances at 97% sequence similarity for bacterial and eukaryotic taxa and determined the phylogenetic identity of OTUs with the SILVA database.

Lake Bloom and Bust Bacterial Communities

To analyze the bacterial composition of HABs, we classified lake communities into three classifications based on cyanobacteria abundance and cell number-bloom, bust, or static. Cyanobacteria cell counts were performed on a fourth composite sample that we collected in a similar method as all our other samples (three 1 L subsamples from the surface to a depth of 30 cm) for the Utah Division of Water Quality's HAB monitoring system in 2017. Blooms were

samples containing at least a cyanobacterial composition of ≥15% of the relative abundance for the entire bacterial community or a cell count greater than 20,000 cells/ml, the Environmental Protection Agency's designation for a HAB (low health risk <20,000 cells/ml, moderate health risk 20,000-100,000 cells/ml, high health risk 100,000-10,000,000, very high health risk >10,000,000). Busts were similar to blooms; however, busts were HABs experiencing a decline in HAB intensity. Samples categorized as busts contained a cyanobacterial composition of ≥15% of the relative abundance of bacterial communities or a cell count greater than 20,000 cells/ml, but the cyanobacterial abundance must be in decline relative to the sample at the previous time step. Static or non-bloom samples contained relatively low levels of cyanobacteria abundance (<15% cyanobacterial abundance) or cells (<20,000 cells/ml). 100 mL from the composite sample was preserved in Lugols solution until samples were analyzed via semi-automated imaging flow cytometry (Phycotech Inc., St. Joseph, MI) within three days. Data were provided by the Utah DWQ (https://goo.gl/dtk7Ri).

To characterize variability in HAB bacterial community, we used Principal Coordinates Analysis (PCoA) based on a Bray-Curtis distance matrix with the 'phyloseq' package in R (McMurdie and Holmes, 2013; Team, 2017). While the PCoA aided in the visualization of communities, we tested for the main effects and among the three HAB communities using pairwise permutational multivariate analysis of variance (PERMANOVA, Anderson, 2001) and the Holm method to correct for multiple comparisons with the 'phyloseq' package in R(Arbizu, 2019). The ordination was visualized using ggplot2 (Wickham, 2016). To evaluate community differences further, we calculated the relative recovery of OTUs and the abundance of 15 families in rDNA communities to identify differences in the distribution of major taxonomical groups (recovery ≥ 1.0%) among each lake and HAB community levels (i.e., bloom, bust,

stationary). Taxonomic trends were shown with a heat map with hierarchal clustering using the *heatmap* function in the 'gplot` package in R (Warnes et al., 2019).

Top-Down Eukaryotic Grazers

We analyzed the relative abundance of eukaryotic grazers to inform our modelling efforts to predict top-down controls on cyanobacterial blooms and busts in each lake. 18S rRNA gene sequences from the Sequences Illumina sequence reads were analyzed within QIIME (v. 1.9.1), an open-source software pipeline suitable for microbial community analysis (Caporaso et al., 2010). We removed barcodes and primers with a custom, in-house script previous to joining paired-end reads by using fastq-join under default parameters (Aronesty, 2011). Joined reads were then de-multiplexed and checked for chimeras (Edgar et al., 2011). We then clustered the de-multiplexed reads into OTUs, applying a similarity threshold of 97%, using QIIME's default OTU clustering tool-uclust (Edgar et al., 2011). Taxonomies of representative OTUs were assigned using uclust and the 18S rRNA gene SILVA 128 database which was clustered into OTUs at 97% similarity (Quast et al., 2013). We calculated the relative recovery of the OTUs, separated grazers into and six groups based on order-level taxonomical differences, and evaluated the taxonomic differences between the lakes and HAB communities in a heat map with hierarchal clustering based *heatmap* function in the 'gplot` package in R (Warnes et al., 2019).

Predicting Top-Down and Bottom-Up Triggers of Cyanobacterial Blooms and Busts

To identify top-down and bottom-up controls on cyanobacterial blooms and bust over the spring and summer, we created generalized least squared models and used hierarchical selection technique for the three dominant cyanobacteria in each lake. A hierarchical model selection is a

statistical method used to parse through variables with the goal to remove uninformative parameters from models. For a given lake, a model was constructed to analyze top-down and bottom-up effects of the three top cyanobacterial species and models for bloom and bust conditions. Therefore, we created thirty-three unique models for Utah Lake and Deer Creek. It should be noted that for the Deer Creek samples, we only had sufficient data to model blooms. Due to insufficient data points, we were unable to model bloom or busts on the Salt Lake bacterial communities. We grouped the bottom-up variables into three categories, macronutrients (i.e., TP, TDP, SRP, PP, DOP, NH_4^+, NO_3^- TDN, and DOC), micronutrients (i.e., B, Ca, Cu, Fe, K, Mg, Mn, S, and Zn), and lake physiochemical properties (i.e., secchi depth, total depth, and temperature, DO, conductivity, and pH). Due to the wide range of scaling in the variables, we scaled the bottom-up variables into Z scores using the scale function in the base R package. For each group, we used the dredge function from the 'MuMIn' package (Bartoń, 2019) to select the best model based on AICc. AICc is a corrected AIC value that adjusts for multiple comparisons. The variables in the best model for each bottom-up group (macronutrients, micronutrients, and lake properties) were compiled into a final model for each of the cyanobacterial species. We then used the dredge function on the final model to select the best model based on AICc. The top-down models had one group that contained the following variables: *Calanoida*, *Phyllopoda*, *Ploimida*, *Monogononta*. Given that there were only four parameters in the top-down model, we only used one model selection to find the best model based on AICc. All models were checked for multicollinearity using the *cor* function in the 'ltm' package in R (Rizopoulos, 2018) to ensure that collinear variables were not modeled together. To account for autocorrelation of time across repeated sampling at the same sites, we used the corAR1 error structure in the 'nlme' R

package. When collinearity emerged between variables, we separated the variables into unique

models which lead to multiple models generated to predict the blooms or bust of specific species.

RESULTS

Bioavailable N and P Varied by Season and Across Lakes

N (NH_4^+ and NO_3^-) and P (SRP) concentrations varied drastically between the hypersaline

and freshwater lakes. P concentrations were highest at Great Salt Lake (TP, 0.79 mg/L ± 0.12,

SRP 0.15 mg/L ± 0.032). Utah Lake and Deer Creek had different TP concentrations (0.037

mg/L ± 0.002 and 0.11 mg/L ± 0.015 respectively) but had similar concentrations of bioavailable

P (SRP, 0.01 mg/L ± 0.001 and 0.019 mg/L ± 0.001 respectively) (Table 1, 2). TP concentrations

on Utah Lake were influenced by site, however, SRP concentrations remained similar across all

sites for each lake. The mouth of Provo bay site on Utah Lake consistently had nearly 2-times

(0.189 mg/L ± 0.023) the availability of TP than the rest of the sites. All forms of P except for PP

on the Great Salt Lake increased over the summer with the highest values captured in 1.2 mg/L

of TP.

NO_3^- and NH_4^+ concentrations were similar between Great Salt Lake (Table 3) and Deer

Creek (NO_3^-, 0.024 mg/L ± 0.04 , 0.2 mg/L ± 0.017; NH_4^+, 0.25 mg/L ± 0.06, 0.19 mg/L ± 0.06

respectively), however, Utah Lake had significantly lower concentrations (NO_3^- , 0.14 mg/L ±

0.001; NH_4^+ , 0.037 mg/L ± 0.009). Of potential bioavailable N, nitrate concentrations on Deer

Creek varied greatly across time with late summer waters having up to 10-times more nitrate

concentrations. Surprisingly, ammonium concentrations do not vary. Nitrate and ammonium

concentrations on the Great Salt Lake varied but with no consistent trend.

Micronutrients Varied Across Lakes

Micronutrient concentrations (B, K, Mn, S) did not vary by site within each lake, however, the concentrations drastically varied between the hypersaline and two freshwater lakes. The Great Salt Lake consistently had higher concentrations of B (1.83 mg/L ± 0.63), K(250 mg/L ± 116), Mn(0.04 mg/L ± 0.02), and S (346 ± 142) than Utah Lake(B, 0.31 mg/L ± 0.01; K, 19.8 mg/L ± 0.8; Mn, 0.02 mg/L ± 0.001; S, 11.8 mg/L ± 0.8) and Deer Creek (B, 0.04 mg/L ±0.004; K, 2.2 mg/L ± 0.2; Mn, 0.01 mg/L ± 0.001; S, 11.7 mg/L ± 0.8). Concentrations of Mn, K, and S on the Great Salt Lake increased over time, whereas the same micronutrients on Deer Creek and Utah Lake did not exhibit any trend across time.

Bloom Composition and Bloom Duration Varied Across the Three Lakes

Regardless of differing nutrient designation and salinity levels, all three lakes experienced at least one bloom event, but the blooms varied in duration and cyanobacterial species composition. Utah Lake experienced 18 bloom events across all seven sampling locations and ranged in duration from one to six week at the beginning of the summer and continuing through fall.(Figure 1 and Table 4) One location, Vineyard, experienced the longest bloom, which lasted six weeks while Bird Island experienced the most blooms with four separate bloom events, none of which lasted more than three weeks. *Aphanizomenon* strain MDT14a was the dominant cyanobacterial species for every bloom on Utah Lake, consistently accounting for upwards of 44.16% of the entire bacterial community. During periods of non-bloom conditions, a variety of Cyanobacteria were present possessing variable relative abundances (4.9% ± 0.48%): *Microcystis sp.* (0.45% ± 0.55), *Aphanizomenon* strain MDT14a (2.9% ± 0.38%), *Aphanizomenon* strain NIES81 (0.17% ± 0.038%), and *Dolichospermum sp.* (0.53% ± 0.16%).

Deer Creek Reservoir experienced one length bloom event at the Charleston location towards the end of the summer with the bloom lasting at least six weeks and was still apparent at our last sampling date. *Phormidiaceae sp.* (8.5 ± 6.1%) and *Microcystis sp.* (9.7 ± 4.7%) were the most abundant cyanobacteria in the Deer Creek bloom. Great Salt Lake experienced four distinct blooms across three different sites during two summer months each lasting one to three weeks. *Nodularia sp.* (9.7 ± 2.1) was the dominant cyanobacteria species comprising the bloom.

Interaction Between Time and HAB Designation (i.e., Bloom, Bust, or Static) Structured Bacterial Communities

In two of the three lakes, Utah Lake and Deer Creek Reservoir, season, followed by HAB designation, structured the bacterial communities. In Utah Lake and Deer Creek, time, or more explicitly season-spring and summer, separated communities along axis one explaining 26% in Utah Lake and 33% in Deer Creek, while bloom and bust communities grouped together away from static communities along axis two in ordination space (variation explained Utah Lake = 11%, Deer Creek 21%) (Figures 2,3). The PERMANOVA results supported the ordination with the interaction between time and HAB designation (two-way PERMANOVA, Utah Lake F = 3.8, R^2 = 0.05, $P < 0.001$; Deer Creek Reservoir F = 1.7, R^2 = 0.04). HAB designation structured bacterial communities in two of the three lakes. Farmington Bay bacterial communities were only influenced by time (one-way PERMANOVA, F = 4.1, R^2 = 0.19, $P = 0.03$) (Figure 4). All bacterial community inferences were based on 164 samples with 9,929,972 total sequences rarefied to 15,000 sequences per sample, and 20,965 unique OTUs with samples possessing an average sequencing coverage of 97.0% ± 0.07 Four samples were removed because they had fewer than 15,000 sequences.

Salinity and Cyanobacterial Blooms and Busts Influenced Bacterioplankton Communities

Between the hypersaline and freshwater lakes, there were robust taxonomical differences in abundant active and dormant taxa, regardless of blooms (Figure 5). In the Great Salt Lake (salinity, 13.8% ± 3.3%), four families, dominated the bacterioplankton community. For example, the relative abundance of the Nostocaceae (Cyanobacteria, hypersaline = 23% ± 7.5, the two freshwater = 0.86% ± 0.84) Microbacteriaceae (Actinobacteria, hypersaline = 23% ± 7.5, the two freshwater = 0.86% ± 0.84), Cyclobacteriaceae (Bacteroidetes, hypersaline = 13% ± 7.6, the two freshwater = 0), and Rhodobacteraceae (Alphaproteobacteria, hypersaline = 2.0% ± 0.68, the two freshwater = 0.49% ± 0.28) were at least 26-times higher in Great Salt Lake than in Utah Lake (salinity, 0.85% ± 0.01) and Deer Creek (salinity, 0.16% ± 0.002) Freshwater lakes contained one family, the Sporichthyaceae (Actinobacteria), that dominated the Utah Lake and Deer Creek communities (the two freshwater = 0%, hypersaline = 13% ± 7.6). Deer Creek bloom and bust communities grouped together with the two Cyanobacterial families, Phormidiaceae and Microcystaceae, accounting for 13% ± 7.6 and 13% ± 7.6 of the bacterioplankton community. Alternatively, the Nostocaceae family (13% ± 7.6), was abundant in Utah Lake blooms and busts.

Utah Lake Eukaryote Communities Remain Stable Regardless of Cyanobacterial Blooms

Eukaryote communities were dominated by three groups, Ceratium (26.2% ± 3.9), Calanoida (16.0% ± 3.6), and Cryptomonas (9.2% ± 1.4). Bloom status does not seem to affect the relative abundance of the eukaryotic communities. All eukaryotic community inferences were based on 88 samples with 5,341,891 total sequences rarefied to 18,000 sequences per sample, and 9,623 unique OTUs with samples possessing a mean sequencing coverage of 98.4% ± 0.001.

Bottom-up Resources Regulated Cyanobacterial Blooms

Nutrient resources influenced the relative abundance of the most abundant cyanobacteria more than the top-down controls (Table 5). The three most abundant cyanobacteria in Utah Lake were *Aphanizomenom* strain MDT14a, *Microcystis sp.*, and *Dolichospermum sp*. During the spring and summer, blooms, increases in relative abundance, of *Aphanizomenom* strain MDT14a was positively correlated with temperature ($P < 0.028$) and the concentration of K ($P = 0.007$). As *Aphanizomenom* abundances decreased multiple times during the season, the decline in this species abundance was negatively correlated with increases in conductivity ($P = 0.0088$) explaining 30% of bust dynamics. The bloom model for *Microcystis* blooms explained more than 50% of the species rise in relative abundance that was positively correlated with increasing levels of SRP ($P < 0.001$) and negatively correlated with higher Ca concentrations ($P = 0.008$) and PP ($P = 0.008$). Busts of *Microcystis* were related to decreases in nitrate ($P = 0.06$) and lower total lake depths ($P = 0.03$), which explained 34% of the N-fixer's decline. During periods of decline, *Dolichospermum sp.* relative abundance was negatively correlated with higher levels of nitrate ($P = 0.005$) and positively correlated with increasing Mn concentrations ($P < 0.001$, model explaining 31% of species variability). HABs on Deer creek were composed of two of the same species as Deer Creek, *Aphanizomenon* and *Microcystis sp.*, and a new Phormidiaceae species were influenced by bottom-up controls, albeit species never reached the immense cyanobacterial community dominance as apparent in Utah Lake. During blooms of the *Phormidiaceae sp.* relative abundance was negatively correlated with higher levels of TDN ($P = 0.01$-0.001) and Mg ($P = 0.01$) and positively correlated with higher S concentrations ($P = 0.007$). Two models were constructed to describe *Phormidiaceae* blooms due to collinearity among the micronutrients. The model predicting blooms of *Microcystis* explained 19% of the species

variation and was positively correlated with increases in B. Unlike the shallow Utah Lake, blooms of the same species of *Aphanizomenom* in Deer Creek were marginally negatively related to total depth ($P = 0.10$), with this one variable describing 21% of the species variation. There were no significant models explain the busts of any cyanobacterial species in Deer Creek.

Top-Down Grazers Tracked the Blooms of the Dominant Species and the Busts of All Cyanobacteria

Top-down controls were only evident in the distribution of our most dominant cyanobacteria, *Aphanizomenon sp.*, in Utah Lake. The blooms of *Aphanizomenon* were positively associated with an increase in the relative abundance of the *Ploimida* species ($P = 0.007$). Additionally, when all cyanobacterial abundance was combined and modelled for Utah Lake busts of cyanobacterial abundance was positively influenced by higher levels of *Monogononta* ($P = 0.04$). another class of rotifers consisting of seven OTUs. Both grazer models explained a substantial amount of the variation in the cyanobacteria involved, roughly 15%. There were no other significant top-down models for the other two lakes.

DISCUSSION

Bioavailable Forms of P and N Elicit Blooms

Our hypothesis that more bioavailable forms of P and N regulate species-specific blooms proved to be overly simplistic. Blooms of *Microcystis sp*. and *Phormidiaceae sp.* were stimulated by SRP, while no one form of P alone triggered *Dolichospermum sp.*, which was activated by TP, and no form of P related to the most abundant cyanobacterial bloomer, *Aphanizomenon sp*. Nostocales species *Dolichospermum* and *Aphanizomenon* bloom dominance are correlated with

increasing total phosphorous concentrations (Andersson et al., 2015). Although *Dolichospermum* was positively correlated with TP, *Aphanizomenon* did not follow the same trend. It is possible that this specific strain of *Aphanizomenon* has different nutrient requirements than other strains of *Aphanizomenon*. These results implicate that all forms of phosphorous have the potential to cause species specific blooms. Internal P storage of nutrient rich lakes will drastically affect the availability of each form of P. However, nutrient cycling of P occurs at different rates depending on its form.

We expected the availability of bioavailable forms of N to regulate the abundance of non-heterocyst species due to their inability to fix nitrogen. *Blooms of Phormidiaceae sp.*, a filamentous cyanobacteria that lacks heterocysts, were positively correlated with TDN while blooms of *Dolichospermum sp.*, a heterocystous cyanobacteria, were negatively correlated with nitrate. It is generally thought that N is not limiting for heterocystous cyanobacteria because they are able to fix nitrogen from the atmosphere. However, forming heterocysts and performing nitrogen fixation is a taxing process. N-fixation cannot support the needs of the system to maintain a cyanobacterial population (Paerl and Otten, 2013) Therefore, it is possible that as nitrate concentrations decrease, the relative abundance of *Dolichospermum* decreases as well because nitrate was its limiting nutrient. Species specific preferences of nutrients are much more complicated. To predict the growth and decline of individual cyanobacterial species, all forms of N and P should be measured.

Micronutrients Trigger and Intensify Blooms

Contrary to our hypothesis that micronutrients involved in metabolic processes will influence blooms to lesser extent than P and N, multiple cyanobacterial species were stimulated by

micronutrients. On Utah Lake, blooms of *Aphanizomenon* were prompted by higher levels of K, but not N or P. In the absence of K, *Aphanizomenon* forms akinetes, small fungus like spores, to go into dormancy (Sukenik et al., 2013). K prevents *Aphanizomenon* from going into dormancy and may potentially break dormancy leading to blooms. These findings suggest that micronutrients are potentially as effective as macronutrients to control bloom species abundances.

Top-Down Controls Only Found with Busts with Non-Selective Grazing

Our hypothesis that top-down selective grazing curbs the growth of specific species was incorrect. None of our models indicated that individual species were targeted by any specific grazer. However, busts of total cyanobacterial abundance were influenced by Monogononta, a rotifer species. The ability of zooplankton to graze on cyanobacteria greatly affected by physiological traits of the zooplankton. Often successful grazing depends on prey selection and the ability to avoid ingesting toxins or toxic cells if the zooplankton does not have tolerance to the toxin (Gilbert and Durand, 1990). Rotifers are sensitive to toxins and selectively graze the non-toxic species (Kirk and Gilbert, 1992). Potentially the Monogononta either avoided toxic cyanobacterial cells but still grazed cyanobacteria indiscriminately or many of our cyanobacterial species were mostly non-toxic. The most abundant cyanobacteria on each lake, *Aphanizomenon*, Nodularia, and *Microcystis* are all capable of producing toxins. According to limited toxin data for Utah Lake provided by the Utah Division of Water Quality, microcystin levels varied between 4-2,000 µg/L at several sampling sites. This suggest that is more likely that Monogononta was able to selectively graze the non-toxic cyanobacteria while avoiding toxin ingestion.

19

CONCLUSION

Bottom-up controls exhibit more influence over Cyanobacteria bloom dynamics than top-down controls. The form of nutrient, specifically N or P, influences the constituents of a Cyanobacteria bloom due to variability of nutrient preferences among the Cyanobacteria. These nutrient preferences essentially dictate the ability of the Cyanobacteria to proliferate and become dominant members of the community. Furthermore, micronutrients may potentially have greater influence on bloom dynamics than previously thought. Specific micronutrients such as K, allow Cyanobacteria to break dormancy and perform essential metabolic functions. To verify this claim, Cyanobacterial communities need to be evaluated with varying levels of micronutrients. Understanding these relationships will shed a greater light on bloom dynamics and may potentially highlight the underlying causes of the initiation, sustaining, and curtailing of Cyanobacteria blooms.

LITERATURE CITED

Abbott, B. W., Moatar, F., Gauthier, O., Fovet, O., Antoine, V., and Ragueneau, O. (2018).

Trends and seasonality of river nutrients in agricultural catchments: 18years of weekly

citizen science in France. *Sci. Total Environ.* 624, 845–858.

doi:10.1016/j.scitotenv.2017.12.176.

Anderson, M. J. (2001). A new method for non-parametric multivariate analysis of variance.

Austral Ecol. 26, 32–46. doi:10.1111/j.1442-9993.2001.01070.pp.x.

Andersson, A., Höglander, H., Karlsson, C., and Huseby, S. (2015). Key role of phosphorus and

nitrogen in regulating cyanobacterial community composition in the northern Baltic Sea.

Estuar. Coast. Shelf Sci. 164, 161–171. doi:10.1016/j.ecss.2015.07.013.

Arbizu, P. M. (2019). *Pairwise multilevel comparison using adonis. Contribute to*

pmartinezarbizu/pairwiseAdonis development by creating an account on GitHub.

Available at: https://github.com/pmartinezarbizu/pairwiseAdonis [Accessed July 15,

2019].

Aronesty, E. (2011). *ea-utils: Command-line tools for processing biological sequencing data.*

Durham, NC.

Bartoń, K. (2019). *MuMIn: Multi-Model Inference*. Available at: https://CRAN.R-

project.org/package=MuMIn [Accessed July 16, 2019].

Bonilla, I., Garcia-González, M., and Mateo, P. (1990). Boron Requirement in Cyanobacteria: Its

Possible Role in the Early Evolution of Photosynthetic Organisms. *Plant Physiol.* 94,

1554–1560. doi:10.1104/pp.94.4.1554.

Brooks, B. W., Lazorchak, J. M., Howard, M. D. A., Johnson, M.-V. V., Morton, S. L., Perkins,
D. A. K., et al. (2016). Are harmful algal blooms becoming the greatest inland water
quality threat to public health and aquatic ecosystems? *Environ. Toxicol. Chem.* 35, 6–13.
doi:10.1002/etc.3220.

Caporaso, J. G., Kuczynski, J., Stombaugh, J., Bittinger, K., Bushman, F. D., Costello, E. K., et
al. (2010). QIIME allows analysis of high-throughput community sequencing data. *Nat.
Methods* 7, 335–336. doi:10.1038/nmeth.f.303.

Chan, F., Pace, M. L., Howarth, R. W., and Marino, R. M. (2004). Bloom formation in
heterocystic nitrogen-fixing cyanobacteria: The dependence on colony size and
zooplankton grazing. *Limnol. Oceanogr.* 49, 2171–2178. doi:10.4319/lo.2004.49.6.2171.

Cole, J. R., Wang, Q., Cardenas, E., Fish, J., Chai, B., Farris, R. J., et al. (2009). The Ribosomal
Database Project: improved alignments and new tools for rRNA analysis. *Nucleic Acids
Res.* 37, D141–D145. doi:10.1093/nar/gkn879.

Descy, J.-P., Leprieur, F., Pirlot, S., Leporcq, B., Van Wichelen, J., Peretyatko, A., et al. (2016).
Identifying the factors determining blooms of cyanobacteria in a set of shallow lakes.
Ecol. Inform. 34, 129–138. doi:10.1016/j.ecoinf.2016.05.003.

Downs, T. M., Schallenberg, M., and Burns, C. W. (2008). Responses of lake phytoplankton to
micronutrient enrichment: a study in two New Zealand lakes and an analysis of published
data. *Aquat. Sci.* 70, 347–360. doi:10.1007/s00027-008-8065-6.

Edgar, R. C., Haas, B. J., Clemente, J. C., Quince, C., and Knight, R. (2011). UCHIME improves
sensitivity and speed of chimera detection. *Bioinformatics* 27, 2194–2200.
doi:10.1093/bioinformatics/btr381.

Foley, J. A., Ramankutty, N., Brauman, K. A., Cassidy, E. S., Gerber, J. S., Johnston, M., et al. (2011). Solutions for a cultivated planet. *Nature* 478, 337–342. doi:10.1038/nature10452.

Ger, K. A., Hansson, L.-A., and Lürling, M. (2014). Understanding cyanobacteria-zooplankton interactions in a more eutrophic world. *Freshw. Biol.* 59, 1783–1798. doi:10.1111/fwb.12393.

Gilbert, J. J., and Durand, M. W. (1990). Effect of Anabaena flos-aquae on the abilities of Daphnia and Keratella to feed and reproduce on unicellular algae. *Freshw. Biol.* 24, 577–596. doi:10.1111/j.1365-2427.1990.tb00734.x.

Haney, J. F. (1987). Field studies on zooplankton-cyanobacteria interactions. *N. Z. J. Mar. Freshw. Res.* 21, 467–475. doi:10.1080/00288330.1987.9516242.

Heisler, J., Glibert, P., Burkholder, J., Anderson, D., Cochlan, W., Dennison, W., et al. (2008). Eutrophication and Harmful Algal Blooms: A Scientific Consensus. *Harmful Algae* 8, 3–13. doi:10.1016/j.hal.2008.08.006.

Kâ, S., Mendoza-Vera, J. M., Bouvy, M., Champalbert, G., N'Gom-Kâ, R., and Pagano, M. (2012). Can tropical freshwater zooplankton graze efficiently on cyanobacteria? *Hydrobiologia* 679, 119–138. doi:10.1007/s10750-011-0860-8.

Kirk, K. L., and Gilbert, J. J. (1992). Variation in Herbivore Response to Chemical Defenses: Zooplankton Foraging on Toxic Cyanobacteria. *Ecology* 73, 2208–2217. doi:10.2307/1941468.

Kozich, J. J., Westcott, S. L., Baxter, N. T., Highlander, S. K., and Schloss, P. D. (2013). Development of a Dual-Index Sequencing Strategy and Curation Pipeline for Analyzing Amplicon Sequence Data on the MiSeq Illumina Sequencing Platform. *Appl. Environ. Microbiol.* 79, 5112–5120. doi:10.1128/AEM.01043-13.

McMurdie, P. J., and Holmes, S. (2013). phyloseq: An R Package for Reproducible Interactive Analysis and Graphics of Microbiome Census Data. *PLOS ONE* 8, e61217. doi:10.1371/journal.pone.0061217.

Moisander, P., Steppe, T., Hall, N., Kuparinen, J., and Paerl, H. (2003). Variability in nitrogen and phosphorus limitation for Baltic Sea phytoplankton during nitrogen-fixing cyanobacterial blooms. *Mar. Ecol. Prog. Ser.* 262, 81–95. doi:10.3354/meps262081.

Paerl, H. W., and Fulton, R. S. (2006). "Ecology of Harmful Cyanobacteria," in *Ecology of Harmful Algae*, eds. E. Granéli and J. T. Turner (Springer Berlin Heidelberg), 95–109. doi:10.1007/978-3-540-32210-8_8.

Paerl, H. W., and Otten, T. G. (2013). Harmful Cyanobacterial Blooms: Causes, Consequences, and Controls. *Microb. Ecol.* 65, 995–1010. doi:10.1007/s00248-012-0159-y.

Pinay, G., Peiffer, S., De Dreuzy, J.-R., Krause, S., Hannah, D. M., Fleckenstein, J. H., et al. (2015). Upscaling Nitrogen Removal Capacity from Local Hotspots to Low Stream Orders' Drainage Basins. *Ecosystems* 18, 1101–1120. doi:10.1007/s10021-015-9878-5.

Pruesse, E., Quast, C., Knittel, K., Fuchs, B. M., Ludwig, W., Peplies, J., et al. (2007). SILVA: a comprehensive online resource for quality checked and aligned ribosomal RNA sequence data compatible with ARB. *Nucleic Acids Res.* 35, 7188–7196. doi:10.1093/nar/gkm864.

Quast, C., Pruesse, E., and Yilmaz, P. (2013). The SILVA ribosomal RNA gene database project: improved data processing and web-based tools. *Nucleic Acids Res* 41.

Quince, C., Lanzen, A., Davenport, R. J., and Turnbaugh, P. J. (2011). Removing Noise From Pyrosequenced Amplicons. *BMC Bioinformatics* 12, 38. doi:10.1186/1471-2105-12-38.

Randall, M. C., Carling, G. T., Dastrup, D. B., Miller, T., Nelson, S. T., Rey, K. A., et al. (2019). Sediment potentially controls in-lake phosphorus cycling and harmful cyanobacteria in shallow, eutrophic Utah Lake. *PLOS ONE* 14, e0212238. doi:10.1371/journal.pone.0212238.

Rizopoulos, D. (2018). *ltm: Latent Trait Models under IRT*. Available at: https://CRAN.R-project.org/package=ltm [Accessed July 16, 2019].

Sarnelle, O. (1993). Herbivore Effects on Phytoplankton Succession in a Eutrophic Lake. *Ecol. Monogr.* 63, 129–149. doi:10.2307/2937177.

Schloss, P. D., Westcott, S. L., Ryabin, T., Hall, J. R., Hartmann, M., Hollister, E. B., et al. (2009). Introducing mothur: Open-Source, Platform-Independent, Community-Supported Software for Describing and Comparing Microbial Communities. *Appl. Environ. Microbiol.* 75, 7537–7541. doi:10.1128/AEM.01541-09.

Seitzinger, S. P., Mayorga, E., Bouwman, A. F., Kroeze, C., Beusen, A. H. W., Billen, G., et al. (2010). Global river nutrient export: A scenario analysis of past and future trends. *Glob. Biogeochem. Cycles* 24. doi:10.1029/2009GB003587.

Song, H., Xu, J., Lavoie, M., Fan, X., Liu, G., Sun, L., et al. (2017). Biological and chemical factors driving the temporal distribution of cyanobacteria and heterotrophic bacteria in a eutrophic lake (West Lake, China). *Appl. Microbiol. Biotechnol.* 101, 1685–1696. doi:10.1007/s00253-016-7968-8.

Sukenik, A., Kaplan-Levy, R. N., Viner-Mozzini, Y., Quesada, A., and Hadas, O. (2013). Potassium deficiency triggers the development of dormant cells (akinetes) in *Aphanizomenon ovalisporum* (Nostocales, Cyanoprokaryota) [1]. *J. Phycol.* 49, 580–587. doi:10.1111/jpy.12069.

Team, R. C. (2017). R: A language and environment for statistical com-puting. *R Found. Stat. Comput. Vienna Austria*.

Vahtera, E., Conley, D. J., Gustafsson, B. G., Kuosa, H., Pitkänen, H., Savchuk, O. P., et al. (2007). Internal Ecosystem Feedbacks Enhance Nitrogen-Fixing Cyanobacteria Blooms and Complicate Management in the Baltic Sea. *Ambio* 36, 186–194.

Warnes, G. R., Bolker, B., Bonebakker, L., Gentleman, R., Liaw, W. H. A., Lumley, T., et al. (2019). *gplots: Various R Programming Tools for Plotting Data*. Available at: https://CRAN.R-project.org/package=gplots [Accessed July 16, 2019].

Wickham, H. (2016). *ggplot2: Elegant Graphics for Data Analysis*. Springer.

Wood, S. A., Borges, H., Puddick, J., Biessy, L., Atalah, J., Hawes, I., et al. (2017). Contrasting cyanobacterial communities and microcystin concentrations in summers with extreme weather events: insights into potential effects of climate change. *Hydrobiologia* 785, 71–89. doi:10.1007/s10750-016-2904-6.

Work, K. A. (2003). Zooplankton grazing on bacteria and cyanobacteria in a eutrophic lake. *J. Plankton Res.* 25, 1301–1306. doi:10.1093/plankt/fbg092.

Zeglin, L. H. (2015). Stream microbial diversity in response to environmental changes: review and synthesis of existing research. *Front. Microbiol.* 6. doi:10.3389/fmicb.2015.00454.

Zhang, Y., Shi, K., Liu, J., Deng, J., Qin, B., Zhu, G., et al. (2016). Meteorological and hydrological conditions driving the formation and disappearance of black blooms, an ecological disaster phenomena of eutrophication and algal blooms. *Sci. Total Environ.* 569–570, 1517–1529. doi:10.1016/j.scitotenv.2016.06.244.
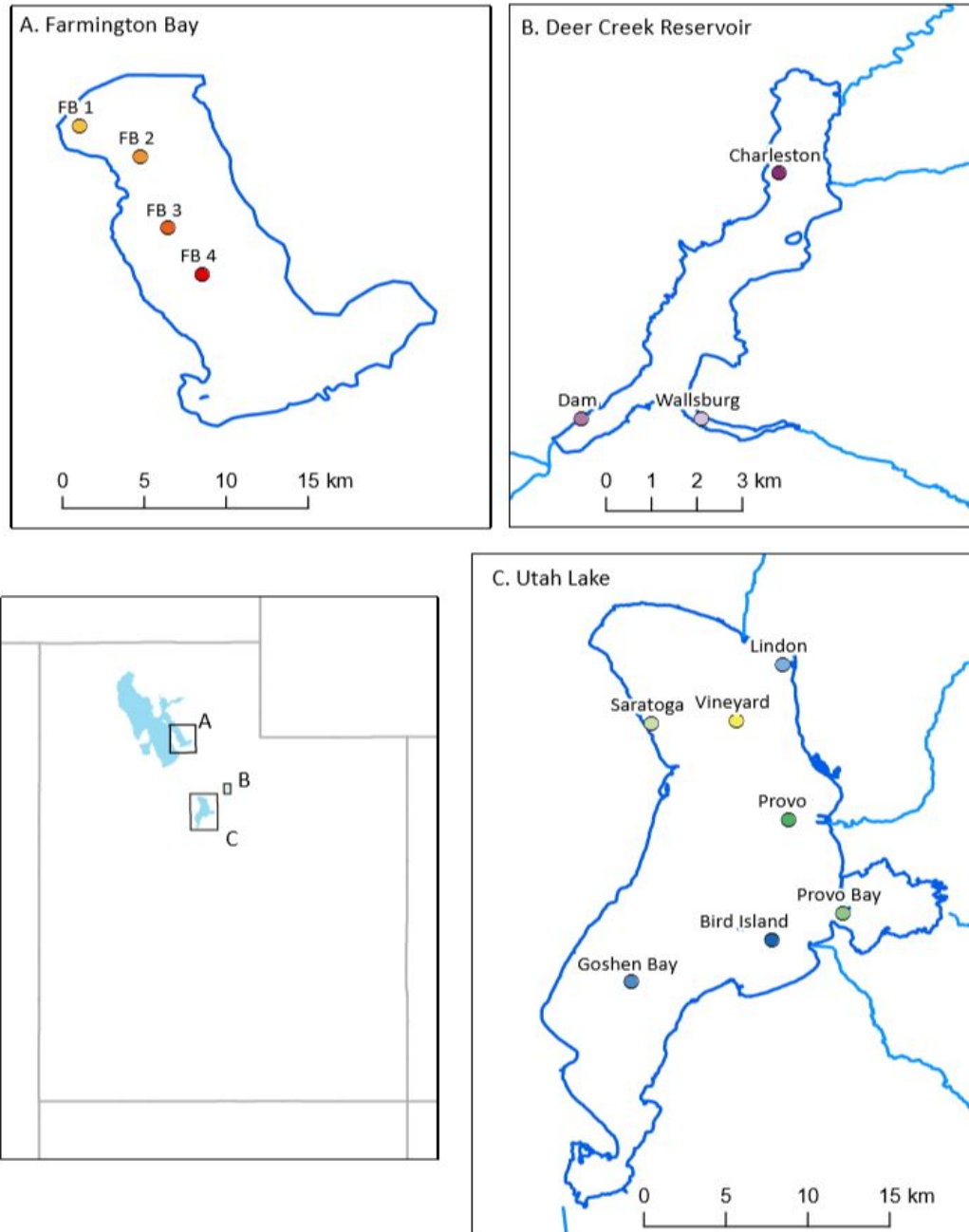
Figure 1. Map of all three lakes with each site plotted. The lower left map shows the location of Farmington Bay in the Great Salt Lake (A), Deer Creek (B), and Utah Lake (C) within the boundaries of the U.S. state of Utah. More detailed maps of sampling points within each lake are shown in the individual maps.
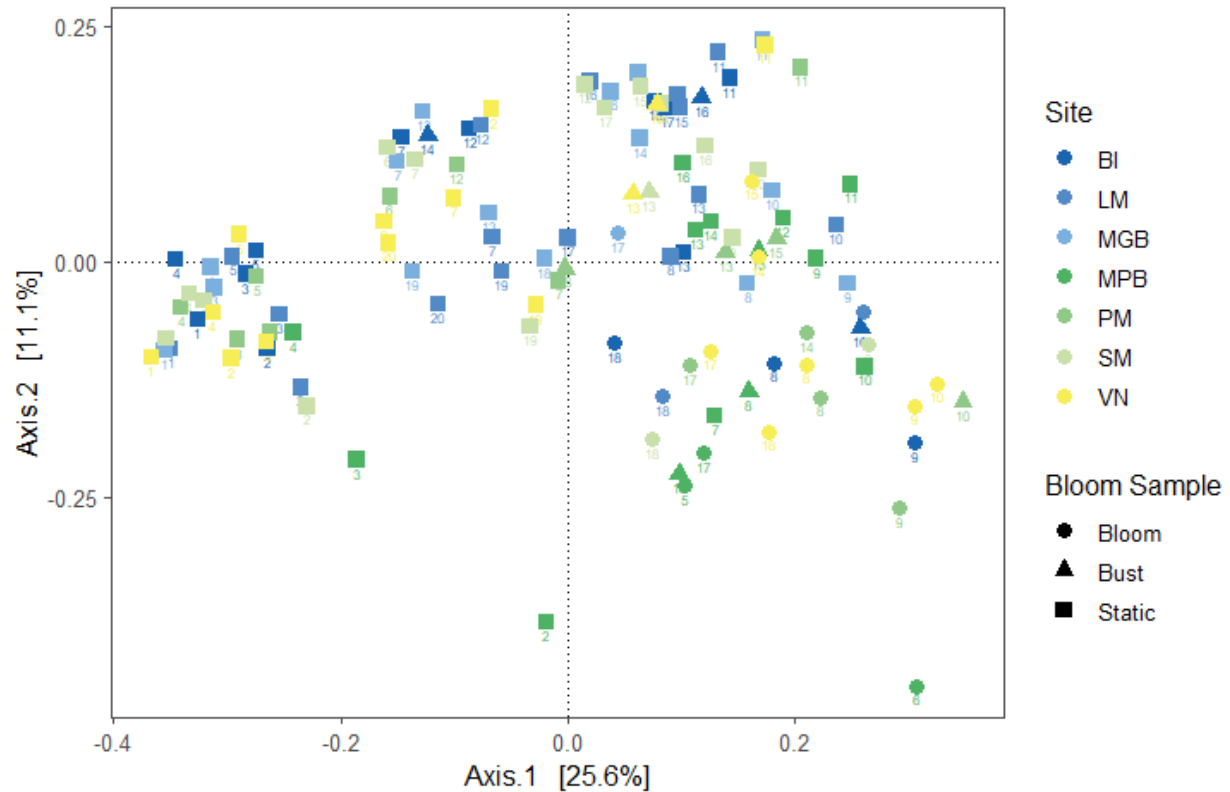
Figure 2 Principal Component Analysis (PCoA) of Utah Lake Bacterial Communities. Time influenced the composition of the communities than any other factor. Time is noted on the PCoA using week numbers. Week 1 corresponds to the first sampling date and the Week 20 corresponds to the last sampling date. Site and Bloom status were also influential factors that affected bacterial community composition.
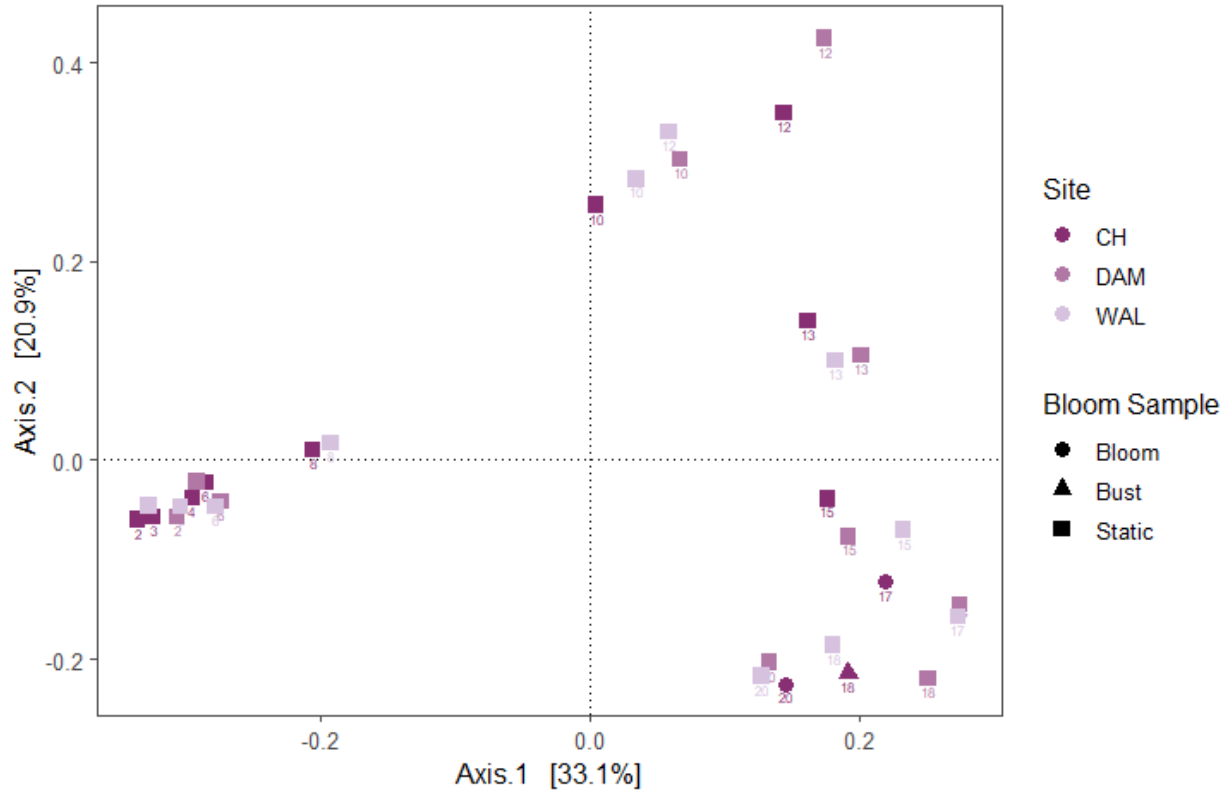
Figure 3. Principal Component Analysis (PCoA) of the Deer Creek Bacterial Communities. Time influenced the composition of the communities than any other factor. Time is noted on the PCoA using week numbers. Week 1 corresponds to the first sampling date and the Week 20 corresponds to the last sampling date.
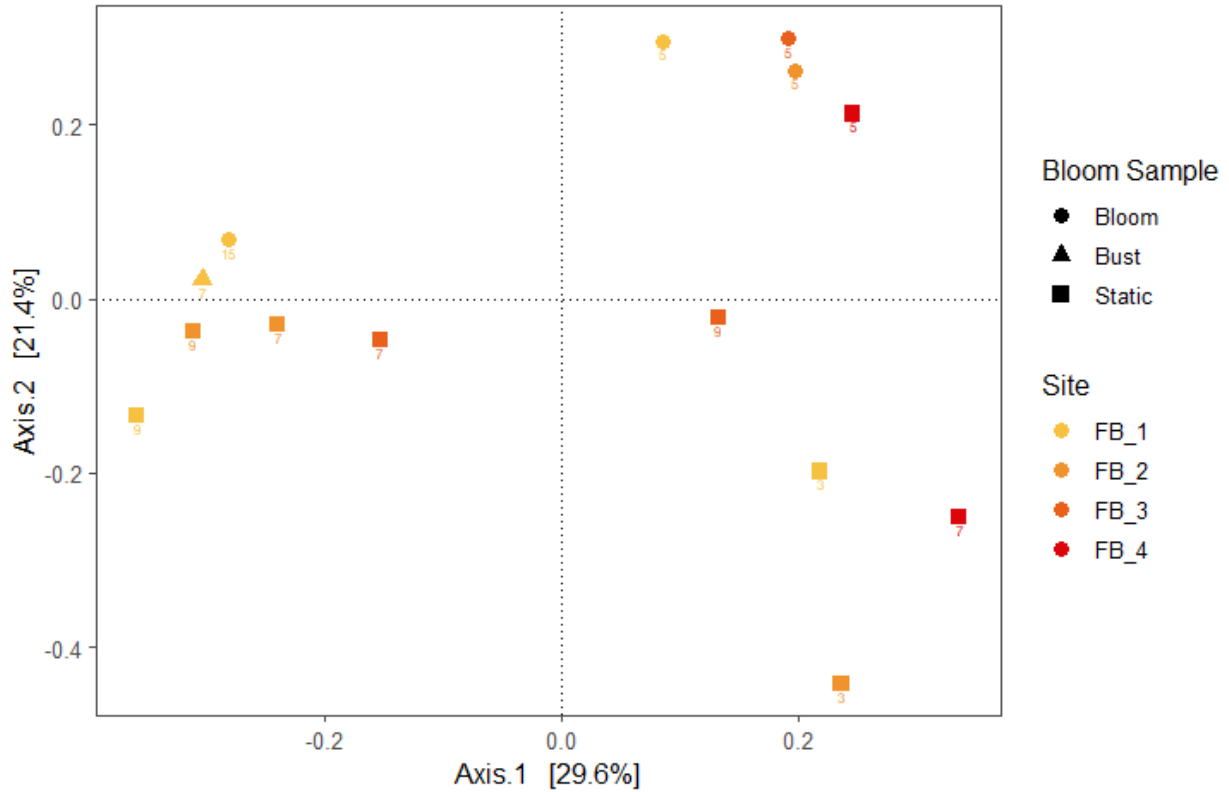
Figure 4. Principal Component Analysis (PCoA) of the Salt Lake Bacterial Communities. Time influenced the composition of the communities than any other factor. Time is noted on the PCoA using week numbers. Week 1 corresponds to the first sampling date and the Week 20 corresponds to the last sampling date.
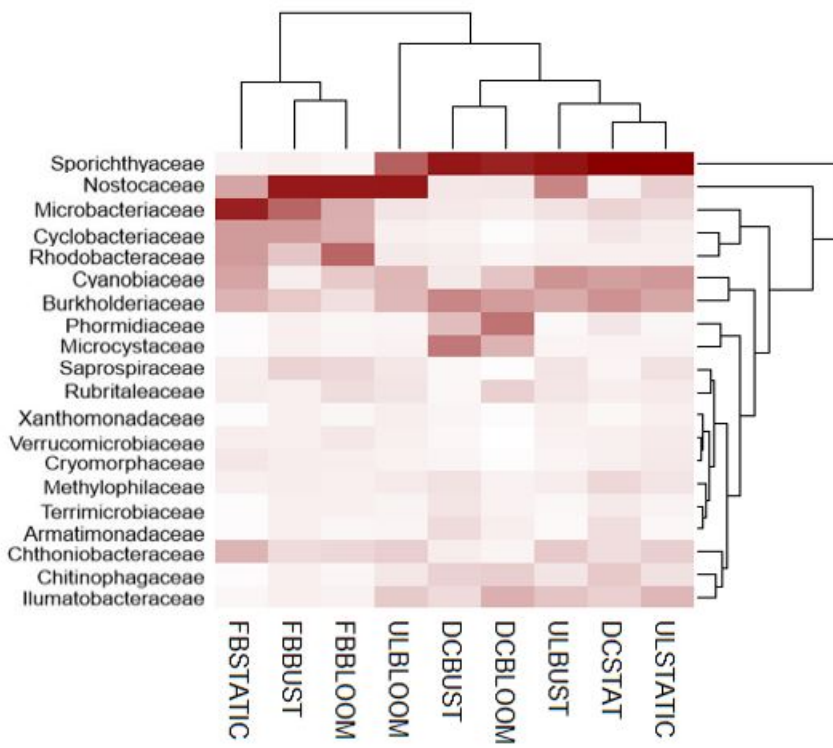
Figure 5. Heatmap of bacterial communities across all 3 lakes.

TABLES

Table 1. Utah Lake General Chemistry. Means and SEMS of every variable measurement for each site on Utah Lake.

Lake	Utah Lake						
Site	Bird Island	Lindon Marina	Mouth of Goshen Bay	Mouth of Provo Bay	Provo Marina	Saratoga Marina	Vineyard Marina
Total Water Depth (m)	2.6 ± 0.03	1.6 ± 0.05	2 ± 0.06	1.4 ± 0.04	2.7 ± 0.03	1.9 ± 0.04	2.3 ± 0.04
Temperature (°C)	21 ± 0.97	22 ± 1.4	23 ± 0.97	21 ± 0.94	22 ± 0.97	20 ± 1.2	20 ± 1.3
Conductivity (µS/cm)	1830 ± 69	1650 ± 60	1670 ± 124	1590 ± 98	1710 ± 66	1710 ± 75	1610 ± 71
Total Phosphorous (mg/L)	0.077 ± 0.008	0.132 ± 0.011	0.089 ± 0.0065	0.189 ± 0.023	0.103 ± 0.001	0.09 ± 0.007	0.084 ± 0.009
Soluble Reactive Phosphorous (mg/L)	0.019 ± 0.003	0.022 ± 0.004	0.016 ± 0.003	0.025 ± 0.005	0.019 ± 0.004	0.016 ± 0.003	0.017 ± 0.003
Particulate Phosphorous (mg/L)	0.056 ± 0.008	0.089 ± 0.016	0.066 ± 0.007	0.16 ± 0.023	0.07 ± 0.008	0.065 ± 0.008	0.051 ± 0.011
Total Dissolved Nitrogen (mg/L)	0.97 ± 0.09	1.4 ± 0.19	0.93 ± 0.08	1.1 ± 0.1	1.1 ± 0.1	1.1 ± 0.12	1.3 ± 0.14

Nitrate (mg/L)	0.16 ± 0.027	0.23 ± 0.051	0.14 ± 0.022	0.05 ± 0.007	0.13 ± 0.022	0.12 ± 0.017	0.15 ± 0.022
Ammonium (mg/L)	0.038 ± 0.007	0.03 ± 0.003	0.029 ± 0.004	0.033 ± 0.007	0.057 ± 0.022	0.033 ± 0.006	0.037 ± 0.006
Boron (mg/L)	0.34 ± 0.007	0.31 ± 0.009	0.33 ± 0.007	0.27 ± 0.016	0.31 ± 0.012	0.32 ± 0.009	0.31 ± 0.011
Calcium (mg/L)	67 ± 3.6	69 ± 3	66 ± 2.7	66 ± 2.6	63 ± 1.9	71 ± 2.8	65 ± 2.7
Potassium (mg/L)	20.8 ± 0.82	19.6 ± 0.73	20.9 ± 0.49	16.8 ± 1.18	20 ± 0.8	20.5 ± 0.68	20.1 ± 0.67
Manganese (mg/L)	0.014 ± 0.001	0.02 ± 0.0021	0.016 ± 0.0016	0.031 ± 0.004	0.017 ± 0.002	0.022 ± 0.002	0.017 ± 0.002
Sulfur (mg/L)	94.5 ± 2.29	86.7 ± 2.01	92 ± 1.56	76.6 ± 3.98	86.9 ± 2.81	90.6 ± 2.3	87.9 ± 1.97

Table 2. Deer Creek General Chemistry. Means and SEMS of every variable measurement for each site on Deer Creek.

Lake	Deer Creek		
Site	Charleston	Dam	Wallsburg
Total Water Depth(m)	8.1 ± 0.55	24.4 ± 1.7	22.2 ± 0.48
Temperature (°C)	19 ± 1.2	18 ± 1.2	19 ± 1.2
Conductivity (µS/cm)	327 ± 17	323 ± 18	337 ± 44
Total Phosphorous (mg/L)	0.04 ± 0.01	0.032 ± 0.007	0.038 ± 0.005
Soluble Reactive Phosphorous (mg/L)	0.01 ± 0.004	0.009 ± 0.004	0.011 ± 0.004
Particulate Phosphorous (mg/L)	0.031 ± 0.01	0.02 ± 0.008	0.025 ± 0.006
Total Dissolved Nitrogen (mg/L)	0.82 ± 0.12	0.83 ± 0.14	0.84 ± 0.14
Nitrate (mg/L)	0.22 ± 0.08	0.19 ± 0.06	0.19 ± 0.06

Ammonium (mg/L)	0.17 ± 0.01	0.15 ± 0.01	0.26 ± 0.11
Boron (mg/L)	0.039 ± 0.008	0.037 ± 0.004	0.032 ± 0.002
Calcium (mg/L)	42.6 ± 2.2	45.7 ± 2.3	44 ± 1.7
Potassium (mg/L)	2.6 ± 0.41	2.1 ± 0.09	2.1 ± 0.12
Manganese (mg/L)	0.011 ± 0.001	0.0087 ± 0.0015	0.0083 ± 0.0006
Sulfur (mg/L)	13 ± 1.5	11.3 ± 0.4	11 ± 0.5

Table 3. Great Salt Lake General Chemistry. Means and SEMS of every variable measurement for each site on the lake.

Lake	Great Salt Lake			
Site	Farmington Bay 1	Farmington Bay 2	Farmington Bay 3	Farmington Bay 4
Total Water Depth(m)	1.03 ± 0.21	0.95 ± 0.26	0.51 ± 0.07	0.52 ± 0.03
Temperature (°C)	21 ± 4	21 ± 6	20 ± 6	16 ± 5
Conductivity (µS/cm)	34618 ± 21065	23818 ± 13957	22010 ± 15832	10040 ± 2689
Total Phosphorous (mg/L)	0.55 ± 0.22	0.71 ± 0.29	0.81 ± 0.15	1.1 ± 0.18
Soluble Reactive Phosphorous (mg/L)	0.07 ± 0.06	0.13 ± 0.08	0.18 ± 0.11	0.22 ± 0.12
Particulate Phosphorous (mg/L)	0.37 ± 0.19	0.24 ± 0.2	0.32 ± 0.2	0.5 ± 0.13
Total Dissolved Nitrogen (mg/L)	3.8 ± 1.2	3.3 ± 0.5	3 ± 0.7	2.8 ± 0.7
Nitrate (mg/L)	0.3 ± 0.32	0.16 ± 0.19	0.3 ± 0.34	0.19 ± 0.18

Ammonium (mg/L)	0.2 ± 0.09	0.33 ± 0.06	0.22 ± 0.07	0.23 ± 0.05
Boron (mg/L)	2.7 ± 1	2 ± 0.9	1.7 ± 0.6	0.9 ± 0
Calcium (mg/L)	87.9 ± 14.4	84.5 ± 11.3	89.9 ± 19.1	91.4 ± 9.5
Potassium (mg/L)	426 ± 185	288 ± 159	208 ± 106	78 ± 14
Manganese (mg/L)	0.02 ± 0.01	0.03 ± 0.03	0.03 ± 0.02	0.07 ± 0.02
Sulfur (mg/L)	552 ± 183	377 ± 184	278 ± 147	175 ± 52

Table 4. General Bloom Information. The number of observed blooms, the total duration of each bloom, and the dominant bloom species of cyanobacteria for sample points in Utah Lake, Deer Creek, and Great Salt Lake during the sampling period of May-Oct, 2019.

Site	Number of Blooms	Total Duration of Blooms (Weeks)	Dominant Bloom Species
Lindon	2	2	AphanizomenonMDT14a
Saratoga	3	3	AphanizomenonMDT14a
Goshen Bay	1	1	AphanizomenonMDT14a
Bird Island	4	7	AphanizomenonMDT14a
Provo Bay	3	6	AphanizomenonMDT14a
Provo	3	8	AphanizomenonMDT14a
Vineyard	2	9	AphanizomenonMDT14a
Charleston	1	3	Phormidiaceae /Microcystis
Dam	0	0	AphanizomenonMDT14a
Wallsburg	0	0	Phormidiaceae
Farmington Bay 1	2	3	Nodularia

Farmington Bay 2	1	1	Nodularia
Farmington Bay 3	1	1	Nodularia
Farmington Bay 4	0	0	Nodularia

Table 5. Bloom and Bust Prediction Models. Bloom and Busts models predict species specific cyanobacterial abundance using a time lag. Bloom and Bust models for Utah Lake and Bloom Models for Deer Creek.

Utah Lake	Equation	AIC	P Value	R^2
Bottom-Up Bloom Models	AphanMDT14a ~ 0.087 + 0.38(K)	211.7	K = 0.0056	0.13
	AphanMDT14a ~ 0.12 + 0.29(Temp)	214.3	Temp = 0.028	0.1
	Microcystis ~ -0.14 - 0.26(Ca) 0.27(PP) + 0.39(SRP)	173.8	Ca = 0.0089 PP = 0.018 SRP = 0.0001	0.39
	Microcystis ~ -0.10 - 0.28(Ca) - 0.26 (SRP)	174.7	Ca = 0.005 SRP = 0.0006	0.34
	Microcystis ~ -0.15 - 0.31(PP) + 0.48(SRP)	177.9	PP = 0.009 SRP = <0.0001	0.32
	Microcystis ~ -0.10 - 0.44(SRP)	177.9	SRP = <0.0001	0.31
	Dolichospermum ~-0.11+ 0.085(TP)	75.7	TP = 0.14	0.046
	Dolichospermum ~-0.12 -0.077(Total Depth)	75.8	Total Depth = 0.097	0.29
	Total Cyano ~0.11 + 0.35(K) + 0.27(Temp) + 0.32(PP)	202.2	K = 0.005 Temp = 0.012 TP = 0.026	0.26
	Total Cyano ~0.1 + 0.36(K) + 0.24(Temp) + 0.33(TP)	201.9	K = 0.004 Temp = 0.024 TP = 0.022	0.27
	Total Cyano ~0.088 + 0.31(Temp)	203.6	Temp = 0.0068	0.13
Top-Down Bloom Models	AphanMDT14a ~ 6.7 + 0.29(Ploimida) + Site	432.9	Ploimida = 0.073	0.14
	Microcystis ~ 0.40 - 0.015(Monogononta)	53.2	Monogononta = 0.45	0.001

	Equation	AIC	P Value	R²
	Dolich ~ 0.22 - 0.10(Monogononta) + Site	290.8	Monogononta = 0.52	0.21
	Total Cyano ~ 8.29 + 0.32(Monogononta) + Site	442.5	Monogononta = 0.6	0.15
Bottom-Up Bust Models	AphanMDT14a ~ -0.11 - 0.36(Conductivity)	67.6	Conductivity = 0.0088	0.16
	Microcystis ~ 1.04 + 1.07(NO3) + 0.46(Total Depth)	89.8	NO3 = 0.064 Total Depth = 0.031	0.34
	Dolichospermum ~ -0.29 - 0.26(NO3) + 0.13(Mn)	3.9	NO3 = 0.005 Mn = 0.0008	0.31
	Total Cyano ~ -0.4620 -0.65(NO3)	65.1	NO3 = 0.072	0.14
Top-Down Bust Models	AphanMDT14a ~ 2.492 + 0.7(Monogononta) + Site	133.7	Monogononta = 0.2051	0.1
	Microcystis ~ 0.78 -0.072(Ploimida)	56.5	Ploimida = 0.16	0.064
	Dolichospermum~ 0.09 + 0.38(Ploimida)	112.6	Ploimida = 0.078	0.14
	Total Cyano ~ 2.04 + 1.05 (Monogononta) + Site	134.9	Monogononta = 0.049	0.15
Deer Creek	**Equation**	**AIC**	**P Value**	**R²**
Bottom-Up Bloom Models	Phormidiaceae ~ 4.7 -12.9(B) - 4.9(DON) + 8.2(NH4)	71.1	B = 0.098 DON = 0.0053 NH4 = 0.54	0.58
	Phormidiaceae ~ 7.0 -4.0(TDN) + 10.8(NH4)	74.7	TDN = 0.0048 NH4 = 0.37	0.58
	Phormidiaceae ~ 8.1 + 22.2(K) - 4.2(NH4)	73.9	K = 0.19 NH4 = 0.71	0.1
	Phormidiaceae ~ 7.5 + 2.6(K) + 11.3(NH4) - 4.0(TDN)	69	K = 0.89 NH4 = 0.37 TDN = 0.013	0.58

	Phormidiaceae ~ 8.3 - 16.1(B) - 4.1(DON) + 32.1(S)	67.8	B = 0.024 DON = 0.0086 S = 0.089	0.68
	Phormidiaceae ~8.9 - 3.5(TDN) - 10.2(B) + 31.8(S)		TDN = 0.0063 B = 0.086 S = 0.089	0.34
	AphanMDT14a ~ 0.15 – 0.75(Total Depth)	51.3	Total Depth = 0.1030	0.21
	AphanMDT14a ~ 1.3 + 5.9(K)	49.3	K = 0.2674	0.08
	AphanMDT14a ~ 0.39 + 1.46(S)	51	S = 0.8113	0.08
	Microcystis ~ 1.01 + 4.8(B)	40.5	B = 0.0024	0.19
	Microcystis ~ 0.58 + 5.311(B) – 2.98(K)	37.3	B = 0.0044 K = 0.4983	0.57
	Total Cyano ~ 0.42 + 0.63(B)	40.5	B = 0.5815	0.24
	Total Cyano ~ 0.79 + 2.5(S)	38.1	S = 0.3420	0.22